



This is a repository copy of *Nonlinear primary and supervisory control of DC microgrids for distributed optimal operation with neighbour-to-neighbour communication*.

White Rose Research Online URL for this paper:

<https://eprints.whiterose.ac.uk/186670/>

Version: Accepted Version

Proceedings Paper:

Michos, G. orcid.org/0000-0002-8138-7475, Baldivieso-Monasterios, P.R. and Konstantopoulos, G.C. orcid.org/0000-0003-3339-6921 (2021) Nonlinear primary and supervisory control of DC microgrids for distributed optimal operation with neighbour-to-neighbour communication. In: 2021 25th International Conference on System Theory, Control and Computing (ICSTCC). 2021 25th International Conference on System Theory, Control and Computing (ICSTCC), 20-23 Oct 2021, Iasi, Romania. Institute of Electrical and Electronics Engineers (IEEE) , pp. 302-307. ISBN 9781665430555

<https://doi.org/10.1109/icstcc52150.2021.9607201>

© 2021 IEEE. Personal use of this material is permitted. Permission from IEEE must be obtained for all other users, including reprinting/ republishing this material for advertising or promotional purposes, creating new collective works for resale or redistribution to servers or lists, or reuse of any copyrighted components of this work in other works. Reproduced in accordance with the publisher's self-archiving policy.

Reuse

Items deposited in White Rose Research Online are protected by copyright, with all rights reserved unless indicated otherwise. They may be downloaded and/or printed for private study, or other acts as permitted by national copyright laws. The publisher or other rights holders may allow further reproduction and re-use of the full text version. This is indicated by the licence information on the White Rose Research Online record for the item.

Takedown

If you consider content in White Rose Research Online to be in breach of UK law, please notify us by emailing eprints@whiterose.ac.uk including the URL of the record and the reason for the withdrawal request.



eprints@whiterose.ac.uk
<https://eprints.whiterose.ac.uk/>

Nonlinear Primary and Supervisory Control of DC Microgrids for Distributed Optimal Operation with Neighbour-to-Neighbour Communication

Grigoris Michos

*Department of Automatic Control
& Systems Engineering
University of Sheffield
Sheffield S102TN, United Kingdom
gmichos1@sheffield.ac.uk*

Pablo R. Baldovieso-Monasterios

*Department of Automatic Control
& Systems Engineering
University of Sheffield
Sheffield S102TN, United Kingdom
p.baldovieso@sheffield.ac.uk*

George C. Konstantopoulos

*Department of Electrical
& Computer Engineering
University of Patras
Rion 26500, Greece
g.konstantopoulos@ece.upatras.gr*

Abstract—In this paper a hierarchical control scheme is proposed for distributed operation of DC Microgrids (MGs) consisting of multiple Distributed Energy Resources (DERs) and local loads with an inherent overvoltage protection for each unit. At the primary control level, the recently proposed state-limiting PI (sl-PI) controller is employed to ensure bounded converter capacitor voltage at all times. At the supervisory control level a non-iterative distributed two-layer MPC approach is proposed, where the system is driven to economic targets calculated according to the load demand. We show the existence of bounds on the voltage dynamics based on ultimate boundedness theory by an appropriate choice of the tuning parameters. Asymptotic stability of the closed loop dynamics is analytically proven and conditions for the recursive feasibility of the supervisory controller are provided based on the inherent robustness properties of nominal MPC. Simulation results are provided to demonstrate the boundedness properties and economic regulation of the proposed control scheme, as well as satisfaction of the operation constraints.

Keywords—Hierarchical Microgrid Control, Distributed Control, Economic Operation, Nonlinear Control

I. INTRODUCTION

During the past decades a surge in the penetration of renewable energy sources (RES) has resulted in a paradigm shift of network operation. The concept of DC MG is a key element of this, as it allows the energy to be distributed directly to consumers and avoid unnecessary AC to DC, and vice versa, conversions [1]. Traditionally, the primary control strategy in DC MGs relies on introducing a virtual resistance at the output of each DER unit, also known as the droop control method [2], [3]. The main disadvantage of droop control is an introduction of an offset from the rated value, which creates the necessity of an additional control level to improve the power sharing, thus reducing unnecessary transmission lines currents [4].

There have been several studies that propose to shift the voltage reference to a desired value by introducing an additional term inside the droop expression. In [5], the proposed method includes a "voltage-shifting" term that reduces voltage deviations from the reference value. This term is calculated as the output of a proportional-integral (PI) controller compensating the error between the converter and the grid voltage.

A voltage-shifting term was also used in [6], with the input to the PI controller being an expression combining local voltage measurements and the average value of the grid DC voltage. In many cases, constraints on the system states as well as an overall economic system operation are required. This necessitates the adoption of optimal control schemes.

The majority of the current optimal techniques utilise some form of information exchange among the entire network in order to calculate the control action, see [7] for a detailed survey. As MGs are power systems that usually span in large geographical areas, transmission of high volume of data in short sampling times is neither practical nor suitable. Therefore, distributed techniques that only use exchange of information among neighbouring subsystems are often desired. Distributed control architectures with neighbour-to-neighbour communication have been proposed in the literature that integrate the Tube MPC to introduce robustness to the system, [8], [9]. The proposed techniques require the computation of complex constraint sets to ensure the recursive feasibility of the distributed MPC, which is usually prohibitively difficult in the presence of nonlinear dynamics.

Aside from voltage regulation and system stability, every DER unit in a DC MG is required to operate within specific voltage limits in order to avoid damage to its components. Different load profiles may result in transients of voltage which could violate converter limits as the authors of [10], [11] suggest. Saturated controllers have been shown to lead in system instability or performance degradation [12]. In light of these issues, a conventional PI controller is inadequate to protect the converter components and more sophisticated control techniques are required.

The contributions of this paper are the following:

- In Section III, we propose a hierarchical control scheme, that incorporates the recently developed sl-PI controller [13] as the primary controller for the voltage dynamics. We leverage on its state limiting properties to establish a bound on the magnitude of the capacitor voltage, thus eliminating any potential damage during transients of the dynamics. Guidelines are provided for tuning the control

parameters to adopt the desired behaviour and achieve asymptotic stability of the equilibria.

- In Section IV, we propose a non iterative distributed two layer supervisory control scheme. For this task, the inherent robustness properties of nominal MPC are exploited, contrary to many linear approaches that utilise some form of Tube MPC. This eliminates the need to calculating complex constraint sets, which can proven to be an arduous task in a nonlinear setting. The upper layer of the proposed scheme computes admissible steady state targets by solving an optimisation problem that represents the economic criteria of the steady state operation. The lower layer computes a control action in a receding horizon manner that minimises the deviation of the state from the targets. The operation constraints of the system take the form of coupled polytopic constraints.
- In Section V, we provide a stability analysis of the closed loop system. Section VI provides the recursive feasibility analysis of the proposed supervisory controller with respect to time-varying information exchanges based on the preview information paradigm of [14].

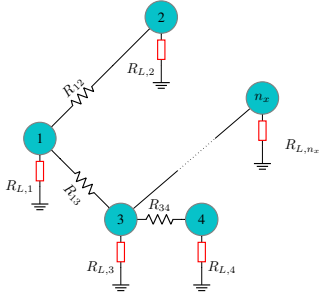


Fig. 1. Generic Meshed DC MG Topology.

A. Notation

A polytope $\mathcal{A} \subset \mathbb{R}^n$ with complexity n_c is characterised by $\mathcal{A} = \{x \in \mathbb{R}^n : Px \leq q\}$ with $P \in \mathbb{R}^{n_c \times n}$ and $q \in \mathbb{R}^{n_c}$. For $x \in \mathbb{R}^n$, $[\cos x] = \text{diag}(\cos x_1, \dots, \cos x_n)$. The N element sequence is $\mathbf{a} = \{a(0), \dots, a(N-1)\}$. A MG can be seen as a graph $\mathcal{G} = (\mathcal{M}, \mathcal{E})$ where the set of nodes \mathcal{M} represent a collection of power converters and local loads; the set of edges $\mathcal{E} \subseteq \mathcal{M} \times \mathcal{M}$ defining the MG topology is characterised by the node-edge matrix $\mathcal{B} \in \mathbb{R}^{|\mathcal{E}| \times |\mathcal{M}|}$ which for edge $e = (i, j) \in \mathcal{E}$ involving nodes i and j can be defined as $[\mathcal{B}]_{ei} = 1$ if node i is the source of $e \in \mathcal{E}$, and $[\mathcal{B}]_{ej} = -1$ if node j is its sink, and zero otherwise.

II. PROBLEM FORMULATION

Consider a DC MG with a set of nodes $\mathcal{M} = \{1, \dots, n_x\}$, see Fig.1, where each node $i \in \mathcal{M}$ represents a DER unit connected to the MG via a DC/DC converter and supplying a local load. The capacitor voltage dynamics of node $i \in \mathcal{M}$ are given by Kirchoff's laws as:

$$C_i \frac{dV_i}{dt} = \iota_i^{\text{ref}} - \iota_i, \quad (1)$$

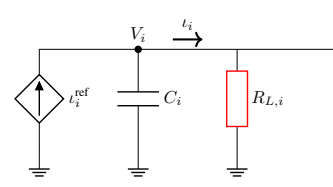


Fig. 2. DC/DC converter connected to a local load and the local bus.

where V_i is the converter voltage, ι_i is the output current, and C_i is the converter output capacitance. It is a common assumption in the literature, see [15], [16] and [17], to consider a faster inner current loop where the inductor current is considered constant to a steady state value ι_i^{ref} , thus simplifying the voltage dynamics analysis. The simplified interlinking DC/DC converter is depicted in Fig.2. The output current ι_i can be expressed as a combination of load and line currents

$$\iota_i = \frac{V_i}{R_{L,i}} + \sum_{j \in \mathcal{N}_i} \frac{V_i - V_j}{R_{ij}}, \quad (2)$$

where $\mathcal{N}_i = \{j \in \mathcal{M} | Y_{ij} \neq 0, i \neq j\}$ is the set of neighbours of the i^{th} node and $Y = \mathcal{L} + D$ is the network admittance matrix with $\mathcal{L} = \mathcal{B}^\top Y_E \mathcal{B}$ being the Laplacian matrix of the graph, Y_E the line admittances, and $D = \text{diag}\left\{\frac{1}{R_{L,i}}\right\}$ the node shunt admittance.

III. PRIMARY CONTROL

In this section the primary voltage control will be presented. In addition, with the use of ultimate boundedness theory we will establish bounds on the voltage dynamics provided the initial state is within the bounded region. The control input of eq.(1) takes the form

$$\begin{aligned} \iota_i^{\text{ref}} &= -k_{p,i} V_i + M_i \sin(\sigma_i), \\ \frac{d\sigma_i}{dt} &= \frac{k_{I,i}}{M_i} (\bar{V} - V_i - m_i \iota_i + \eta_i) \cos(\sigma_i), \end{aligned} \quad (3)$$

with $k_{p,i}$, M_i , $k_{I,i}$ being tuning parameters and \bar{V} the rated voltage. This is a modified version of the sl-PI, introduced in [13], that includes the droop control expression $V_i = \bar{V} - m_i \iota_i$, with m_i being the droop control coefficient. Additionally, a voltage shifting term η_i is supplied by the supervisory controller. The closed loop voltage dynamics are

$$\begin{aligned} C_i \frac{dV_i}{dt} &= -k_{p,i} V_i + M_i \sin(\sigma_i) - \frac{V_i}{R_{L,i}} - \sum_{j \in \mathcal{N}_i} \frac{V_i - V_j}{R_{ij}}, \\ \frac{d\sigma_i}{dt} &= \frac{k_{I,i}}{M_i} (\bar{V} - V_i - m_i \iota_i + \eta_i) \cos(\sigma_i). \end{aligned} \quad (4)$$

Our first result follows,

Proposition 1: For each node $i \in \mathcal{M}$, if

$$|V_i(0)| \leq V^{\max} = \frac{M_i}{k_{p,i}} \quad (5)$$

then $|V_i(t)| \leq V_i^{\max}, \forall t > 0$.

Proof 1: We invoke the C^1 energy function of the capacitor $W_i(V_i) = \frac{1}{2}C_i V_i^2$ with time derivative,

$$\begin{aligned} \frac{dW_i(V_i)}{dt} &= -k_{p,i}V_i^2 + V_i M_i \sin(\sigma_i) + V_i \iota_i, \\ &\leq -k_{p,i}V_i^2 + |V_i| M_i + V_i \iota_i. \end{aligned}$$

To ensure the voltage is bounded we define two cases; (a) $V_i \iota_i \leq 0$ and (b) $V_i \iota_i > 0$. If (a) holds, then

$$\frac{dW_i(V_i)}{dt} \leq -k_{p,i}V_i^2 + |V_i| M_i.$$

Using [18, Theorem 4.18], it can be seen that for $|V_i(0)| \leq \frac{M_i}{k_{p,i}}$ the solution of the voltage dynamics $V_i(t)$ is ultimate bounded with ultimate bound $\frac{M_i}{k_{p,i}}$ for every $t \geq 0$, i.e.

$$|V_i(t)| \leq \frac{M_i}{k_{p,i}}, \forall t \geq 0.$$

In the case of (b), then due to the structure of the network, at least one $j \in \mathcal{M}$ converter should feed the i^{th} load and thus $V_j \geq V_i$. Then, similarly from case (a), $V_i \leq V_j \leq V^{\max}$. For more details, see [15, Section 3A]. Therefore the tuning parameters M_i and $k_{p,i}$ can be chosen to establish an appropriate converter voltage bound $V^{\max} = \frac{M_i}{k_{p,i}}$.

IV. DISTRIBUTED SUPERVISORY CONTROL

The aim of the supervisory control is to drive the system state trajectories to meet the economic criteria while satisfying the operation constraints. To achieve this, the supervisory voltage regulation consists of two layers; an upper layer providing the target steady state values and a lower layer minimising the deviation from the targets in an optimal manner. Each sampling time $k \in \mathbb{N}$, every i^{th} local node transmits its voltage $V_i(k)$ measurement to its neighbours $j \in \mathcal{N}_i$ and the two optimisation problems are solved to provide an input η_i to the local primary controller.

A. Upper Layer

The equilibrium pair of the voltage dynamics $(V_i^{eq}, \sigma_i^{eq})$ can be described by,

$$V_i^{eq} = [1 + m_i Y_{ii}]^{-1} [\bar{V} + \eta_i - m_i w_i], \quad (6)$$

$$\sigma_i^{eq} = \arcsin \left[M_i^{-1} ((k_{p,i} + Y_{ii}) V_i^{eq} + w_i) \right], \quad (7)$$

with $w_i = \sum_{j \in \mathcal{N}_i} Y_{ij} V_j$ representing the transmitted information. The upper layer solves a quadratic programming problem formulated as,

$$\begin{aligned} (V_i^t, \eta_i^t) &= \arg \min_{V_i, \eta_i} \ell_{\text{eco}}(V_i, \bar{V}) \\ &\text{s.t.} \\ V_i &= \frac{\bar{V} + \eta_i - m_i w_i}{1 + m_i Y_{ii}}, \\ V_i &\in \mathcal{S}_i, \end{aligned} \quad (8)$$

where the optimal solution pair $z_i^t = (V_i^t, \eta_i^t)$ is the target that is supplied to the lower layer, ℓ_{eco} is a quadratic function, \mathcal{S}_i is a polytopic constraint representing a collection of operation and economic constraints.

B. Lower Layer

The lower layer consists of local distributed nonlinear MPCs, where each MPC- i is designed to drive the system to the local target z_i^t provided by the upper layer. A receding horizon approach is adopted, where, at each sampling instant k , a finite horizon optimal control problem is solved to calculate an optimal control sequence η_i^o . The first element of this sequence is used as an input to the system, $\eta_i(k) = \eta_i^o(0|k)$. In order to accommodate a distributed approach, the transmitted information is included in the predictions of each MPC- i in the form of a N -length disturbance sequence of equal elements $\mathbf{w}_i(k) = \{w_i(0|k) = w_i(k), w_i(1|k) = w_i(k), \dots, w_i(N-1|k) = w_i(k)\}$. The same information is used to parametrise the operation state constraints $\mathbb{X}_i(w_i)$, formed as polytopic bounded regions of the line currents connected to the i^{th} node. In addition, there are in place uncoupled polytopic input constraints \mathbb{U}_i . Each local MPC- i solves

$$\begin{aligned} P_i^o(V_i, \eta_i, z_i^t, \mathbf{w}_i) &= \\ \min_{\eta_i} &\sum_{n=0}^{N-1} \ell(V_i(n) - V_i^t, \eta_i(n) - \eta_i^t) \\ \text{s.t.} & \\ V_i(0) &= V_i(k) \\ (V_i^+(n), \sigma_i^+(n)) &= \\ &H_i(V_i(n|k), \sigma_i(n|k), \eta_i(n|k), w_i(n|k)), \\ &\forall n \in [0, N-1] \\ (V_i, \eta_i) &\in \mathbb{X}_i(w_i(n|k)) \times \mathbb{U}_i, \forall n \in [0, N-1] \\ V_i(N) &= x_{f,i}. \end{aligned} \quad (9)$$

where $H(\cdot)$ is the discrete version of the closed loop voltage dynamics (4). A consequence of each local MPC perceiving the neighbouring voltages as constant for the entire horizon is that, at sampling instant k , the terminal constraint set $\mathbb{X}_{f,i} := \{x_{f,i} = V_i^t\}$ may be outside the state constraint set $\mathbb{X}_i(w_i)$. However, similar to [19], we can overcome this by forcing the states to converge to the closest to the target admissible state. If the target V_i^t at time k is inside the constraint set, then $\mathbb{X}_{f,i} := \{x_{f,i} = V_i^t\}$. If not, then the terminal set is replaced by the closest admissible steady state target, i.e. $x_{f,i} = \hat{V}_i^t$, with $\mathcal{D}(\cdot)$ a strictly convex distance function and

$$\hat{V}_i^t = \arg \min_{V_i} \{\mathcal{D}(V_i - V_i^t) | V_i \in \mathbb{X}_i(w_i)\}$$

V. STABILITY ANALYSIS

For the stability proof of the node voltages, the entire MG needs to be considered as the node voltage dynamics are coupled via the MG network. In the following expression, k_p , m , k_I , M , C are diagonal matrices with each (i, i) element being the i^{th} node respective parameter value. Considering a steady state equilibrium point (V^{eq}, σ^{eq}) with vector elements $V_i^{eq} \in (0, V^{\max})$ and $\sigma_i^{eq} \in (-\frac{\pi}{2}, \frac{\pi}{2})$ the resulting Jacobian matrix of the system becomes,

$$J = \begin{bmatrix} C^{-1}(-k_p - Y) & C^{-1}M[\cos(\sigma^{eq})] \\ -M^{-1}K_I(I_{n_x} + mY)[\cos(\sigma^{eq})] & 0_{n_x \times n_x} \end{bmatrix}.$$

For any positive k_p , M chosen to satisfy Proposition 1 and any $k_T > 0$ the Jacobian matrix eigenvalues have negative real part and each voltage equilibrium V_i^{eq} is asymptotically stable with region of attraction $[-\frac{k_{p,i}}{M_i}, \frac{k_{p,i}}{M_i}] \times [-\frac{\pi}{2} + \delta, \frac{\pi}{2} - \delta]$, for any arbitrary small $\delta > 0$. For further details on the stability properties of the sl-PI, the reader is referred to [13].

VI. RECURSIVE FEASIBILITY OF THE SUPERVISORY CONTROLLER

In this section we show the recursive feasibility of each MPC-i. We utilise the inherent robustness properties of nominal MPC in order to demonstrate the robustness of the proposed control scheme to errors caused by small perturbations of the transmitted information between sampling instances. In order to simplify the analysis, we employ the discrete time model of the nominal system, that is given by the Euler discretisation as $V_i^+ = H(V_i, f(V_i, \eta_i, w_i)) = V_i + \Delta T f(V_i, \eta_i, w_i)$, where ΔT is the sampling period. It is noted that the evolution of the uncertain system, is given by $V_i^+ = V_i + \Delta T f(V_i, \eta_i, w_i^+)$.

Assumption 1: The value function P_i^o is class- \mathcal{K} continuous on the bounded sets and satisfies

$$|P_i^o(z_1) - P_i^o(z_2)| \leq \mathcal{F}(|z_1 - z_2|),$$

with \mathcal{F} a class- \mathcal{K} function.

This assumption is satisfied for positive closed and compact constraint sets, continuous and convex dynamics over the constraint set and convex continuous cost; for a detailed analysis see [20]. A characterisation of the model error induced by changes in the disturbance sequences between two consecutive sample times k , is obtained by,

$$|\mathbf{w}_i^+ - \mathbf{w}_i| = |\mathbf{w}_i^+ - \mathbf{w}_i| |\mathbb{1}_c|,$$

where $c = N$. This leads to

$$|\mathbf{w}_i^+ - \mathbf{w}_i| = \left| \sum_{j \in \mathcal{N}_i} Y_{ij} (V_j^+ - V_j) \right| \sqrt{c},$$

which, using the discrete model, results in

$$|\mathbf{w}_i^+ - \mathbf{w}_i| = \left| \sum_{j \in \mathcal{N}_i} Y_{ij} \Delta T f_j(V_j, \eta_j, w_j) \right| \sqrt{c}.$$

Finally as $f_j(V_j, \eta_j, w_j)$ is bounded by the MPC-j, i.e. there exists B_j such that $f_j(V_j, \eta_j, w_j) \leq B_j$, then a bound can be derived on the error δw_i between the elements of the two consecutive disturbance sequences as

$$|\delta w_i| \leq \lambda_i,$$

with $\lambda_i = \Delta T \sum_{j \in \mathcal{N}_i} |Y_{ij}| |B_j| \sqrt{c}$.

Assumption 2: The maximum disturbance error δw_i satisfies

$$\lambda_i \leq \mathcal{F}^{-1}((\rho - \gamma)\beta),$$

with $\rho \in (\gamma, 1)$, $\gamma \in (0, 1)$ and positive constant β such that it defines a level set of the value function $\Omega_\beta = \{V_i | P_i^o(V_i, \mathbf{w}_i) \leq \beta_i\}$.

First we establish the recursive feasibility of eq.(9) under unchanging disturbances, i.e. when $\delta w_i = 0$ the state remains within the respective feasible set $\mathcal{X}_N(\mathbf{w}_i) = \{V_i \in \mathbb{X}_i(\mathbf{w}_i) : \mathcal{U}_i(V_i, \mathbf{w}_i)\}$, with $\mathcal{U}_i(V_i, \mathbf{w}_i)$ the set of admissible control sequences.

Proposition 2: Let Assumption 1 hold. If $\mathbf{w}_i^+ = \mathbf{w}_i$ and the terminal set $\mathbb{X}_{f,i}$ is control invariant for the system $H(\cdot)$, then $V_i \in \mathcal{X}_N(\mathbf{w}_i)$ implies $V_i^+ \in \mathcal{X}_{N+1}(\mathbf{w}_i^+)$.

Proof 2: For a fixed disturbance, i.e. $\mathbf{w}_i^+ = \mathbf{w}_i$, the candidate state and control sequences $\mathbf{V}_i(V_i^+, \mathbf{w}_i^+)$, $\boldsymbol{\eta}_i(V_i^+, \mathbf{w}_i^+)$ at time $k+1$ are the tails of the optimal sequences $\mathbf{V}_i(V_i, \mathbf{w}_i)$, $\boldsymbol{\eta}_i(V_i, \mathbf{w}_i)$ at time k , with the addition of the terminal state as the last element, i.e.,

$$\begin{aligned} \mathbf{V}_i(V_i^+, \mathbf{w}_i^+) &= \{V_i^o(1|V_i, \mathbf{w}_i), V_i^o(2|V_i, \mathbf{w}_i), \dots, \\ &\quad V_i^o(N-1|V_i, \mathbf{w}_i), x_{f,i}\}, \\ \boldsymbol{\eta}_i(V_i^+, \mathbf{w}_i^+) &= \{\eta_i^o(1|V_i, \mathbf{w}_i), \eta_i^o(2|V_i, \mathbf{w}_i), \dots, \\ &\quad \eta_i^o(N-1|V_i, \mathbf{w}_i), \eta_i^o(N-1|V_i, \mathbf{w}_i)\}. \end{aligned}$$

Exploiting the properties of the primary dynamics, the terminal set $\mathbb{X}_{f,i} = \{x_{f,i}\}$ is control invariant for the system, as shown in Section V. Therefore, the sequences are feasible and the problem is recursively feasible with $\mathcal{X}_N(\mathbf{w}_i) \subseteq \mathcal{X}_{N+1}(\mathbf{w}_i^+)$. This leads to the next proposition, showing the preservation of the monotonic decent of the cost function, when the disturbance sequence \mathbf{w}_i is permitted to change between sampling times.

Proposition 3: Let $V_i \in \Omega_\alpha(\mathbf{w}_i) = \{V | P_i^o(V, \mathbf{w}_i) \leq \alpha\} \subseteq \mathcal{X}_N(\mathbf{w}_i)$ for some $\alpha \geq \beta > 0$. The set $\Omega_\alpha(\mathbf{w}_i)$ is robust positive invariant for $V_i^+ = H(V_i, \eta_i, w_i + \delta w_i)$ and $V_i \in \Omega_\alpha(\mathbf{w}_i)$ implies $V_i^+ \in \Omega_\alpha(\mathbf{w}_i^+)$.

Proof 3: Using Proposition 2, the value function under the proposed MPC satisfies the monotonic decent property

$$P_i^o(H(V_i, \eta_i, w_i), \mathbf{w}_i) \leq \gamma P_i^o(V_i, \mathbf{w}_i),$$

for all $x \in \mathcal{X}_N(\mathbf{w}_i)$. When $\delta w_i \neq 0$, Assumption 1 allows for the following expression to hold

$$\begin{aligned} P_i^o(H(V_i, \eta_i, w_i + \delta w_i)) - P_i^o(H(V_i, \eta_i, w_i)) \\ \leq \mathcal{F}(|w_i + \delta w_i - w_i|). \end{aligned}$$

From Assumption 2,

$$\begin{aligned} P_i^o(H(V_i, \eta_i, w_i + \delta w_i)) &\leq P_i^o(H(V_i, \eta_i, w_i)) + \mathcal{F}(\lambda_i) \\ &\leq \gamma P_i^o(V_i, \mathbf{w}_i) + (\rho - \gamma)\beta \\ &\leq \gamma\alpha + \rho\alpha - \gamma\alpha \\ &< \alpha \end{aligned}$$

The system state remains within $\Omega_\alpha(\mathbf{w}_i)$, therefore all future states satisfy $V^+ \in \Omega_\alpha(\mathbf{w}_i^+) \subseteq \mathcal{X}_N(\mathbf{w}_i^+)$.

Let $\mathbb{X}_{ij} = \mathbb{X}_i \times \mathbb{X}_j$. The preservation of the monotonic decent property in combination with the admissibility of the terminal constraint leads to Corollary 1.

Corollary 1: If $(V_i, V_j) \in \mathcal{B}_\xi \subseteq \mathbb{X}_{ij}$, with \mathcal{B}_ξ a ball of radius $\xi \geq 0$, the Cartesian product of the neighbouring nodes one-step forward reachable sets is within the coupled constraint set,

i.e. $\mathcal{R}_i \times \mathcal{R}_j \subseteq \mathbb{X}_{ij}$ with $\mathcal{R}_i(V_i(k), \mathbf{w}_i) = \{H(V_i, \eta_i, \mathbf{w}_i) \in \mathbb{R}^n : \eta_i \in \mathcal{U}_i(V_i, \mathbf{w}_i)\}$ and the problem remains feasible for all future times.

VII. SIMULATIONS

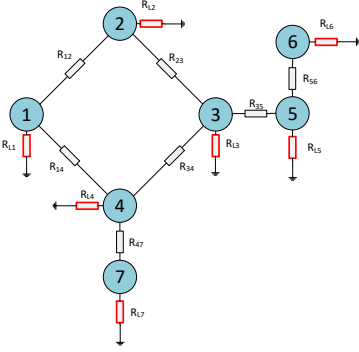


Fig. 3. A network diagram of four converters connected in a circle and each to a local load.

We investigate a network of seven DC/DC converters, each connected to a local load, as depicted in Fig.3. The capacitor steady state voltage economic criteria are to operate close to the rated voltage $\bar{V} = 100V$ without the converter current exceeding a maximum value $i_{\max} = 10A$. In addition, the operation constraints of the system bound the transmission lines power to their respective bound. A quadratic cost function with identity matrices as optimisation weights, $Q = I_{n_x \times n_x}$, $R = I_{m_\eta \times m_\eta}$, is used for the lower layer of the supervisory control. The aim for each local load is to be solely supplied from the respective local converter when the converter current limit can be satisfied, thus reducing the unnecessary line power losses and voltage deviations from the rated voltage. In the case of the load requiring more than i_{\max} , steady state targets are computed where the load is fed by neighbouring nodes while satisfying the economic criteria.

A comparison of the proposed technique is also made with the widely-used Droop-Voltage scheme, where a PI controller is used for the voltage regulation and an additional PI in the supervisory layer penalising deviations from target voltages, see Fig. 6. The target values for the supervisory layer of the droop scheme are the voltage targets that are calculated from the upper control layer of the proposed control scheme.

The system initially is required to satisfy a load demand of $R_L = [13 \ 70 \ 80 \ 40 \ 70 \ 80 \ 40]$, which can be supplied by each local converter at rated voltage and without violating the converter current limit. At time $t = 1ms$ the load changes to $R_L = [9 \ 70 \ 9 \ 40 \ 70 \ 80 \ 40]$ and the voltages are driven to the new targets, with loads R_{L1} , R_{L3} being supplied by converters $i = 1$ and $i = 3$ and the neighbours. Then, at time $t = 2ms$ another load change occurs driving the system to new steady state targets

It is shown that the proposed control scheme is able to satisfy the operation coupled constraints at all times, see Fig.5, and drive the voltages to the desired economic targets Fig. 4. In

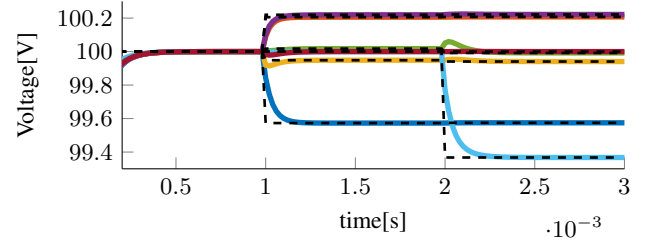


Fig. 4. Converter voltage trajectories of Node 1 (—), Node 2 (—), Node 3 (—), Node 4 (—), Node 5 (—), Node 6 (—), Node 7 (—), and setpoints (---) of all converter subsystems with the use of the proposed control scheme.

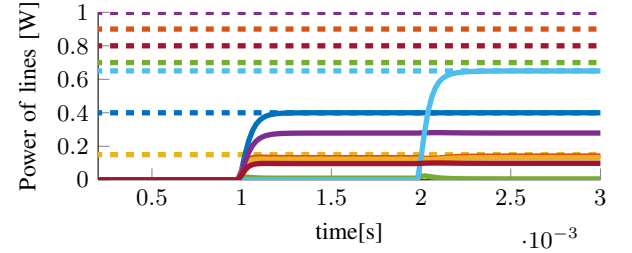


Fig. 5. Line power trajectories using the proposed control scheme and the respective boundaries for *Line*₁₂ (—), *Line*₂₃ (—), *Line*₃₄ (—), *Line*₄₁ (—), *Line*₃₅ (—), *Line*₅₆ (—), *Line*₄₇ (—).

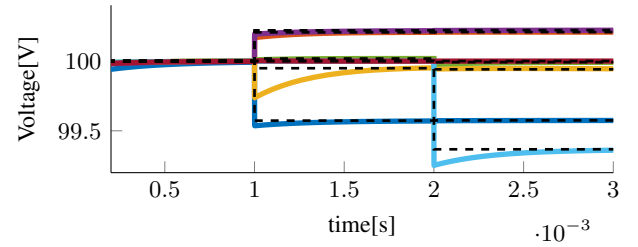


Fig. 6. Converter voltage trajectories of Node 1 (—), Node 2 (—), Node 3 (—), Node 4 (—), Node 5 (—), Node 6 (—), Node 7 (—), and setpoints (---) of all converter subsystems with the use of the Voltage-Droop control scheme.

comparison, the droop-voltage control scheme violates the line constraints Fig. 7. Additionally, it can be seen, in Fig.8, that the proposed control method reduces the total power dissipated in the transmission lines, when compared to the conventional approach.

TABLE I
SYSTEM AND CONTROL PARAMETERS

Parameters	Values
$C[\mu F]$	[.2 .25 .1 .14 .15 .1 .14]
g	200
M_i	6×10^3
$k_{I,i}$	2×10^7
m_i	0.42
[R12,R23,R34,R14,R35,R56,R47][Ω]	[1 1.5 .5 .6 .5 .6 .5]

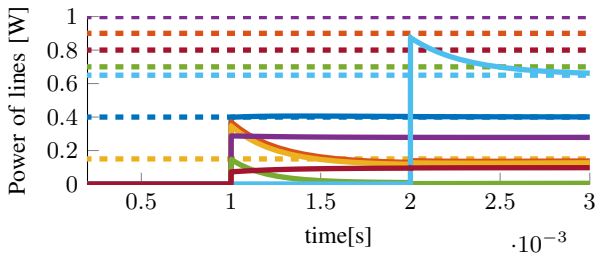


Fig. 7. Line power trajectories using Voltage-Droop control and the respective boundaries for $Line_{12}$ (—, - - -), $Line_{23}$ (—, - - -), $Line_{34}$ (—, - - -), $Line_{41}$ (—, - - -), $Line_{35}$ (—, - - -), $Line_{56}$ (—, - - -), $Line_{47}$ (—, - - -).

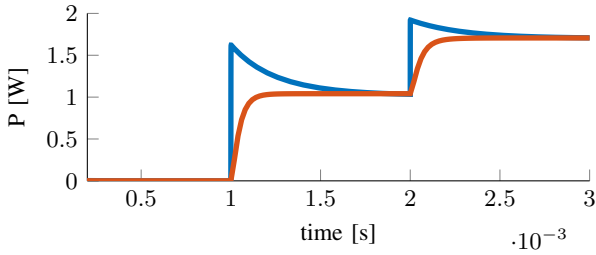


Fig. 8. Total power dissipated in the lines using the proposed (—) and the Voltage-Droop (—) control scheme.

VIII. CONCLUSIONS

In this paper a hierarchical control scheme for DC MGs with multiple DERs and local loads has been proposed, that employs the sl-PI controller at the primary level and a two-layer nonlinear distributed optimal control problem at the supervisory level. The closed loop system is equipped with inherent overvoltage protection of each converter. Reducing voltage deviations from the rated value, coupled constraints satisfaction, and system economic operation is shown, while the optimal control problem is guaranteed to remain feasible at all times.

The aim of this paper was twofold; to introduce state limiting properties in the system dynamics and to present a distributed nonlinear MPC approach for islanded DC MGs that is based on the inherent robustness properties of nominal MPC. Thus, an alternative is introduced to distributed MPC that does not require computation of complex constraints sets. Future research will investigate the effect of nonlinear loads to the proposed scheme and enlargement of the feasible regions of the supervisory controller.

ACKNOWLEDGEMENT

This work is supported by EPSRC under Grants No EP/S001107/1 and EP/S031863/1, and under Grant 81359 from the Research Committee of the University of Patras via “C. CARATHEODORY” program.

REFERENCES

[1] Xia, Y., Wei, W., Peng, Y., Yang, P. and Yu, M., 2017. Decentralized coordination control for parallel bidirectional power converters in a

grid-connected DC microgrid. *IEEE Transactions on Smart Grid*, 9(6), pp.6850-6861.

[2] Schiffer, J., Seel, T., Raisch, J. and Sezi, T., 2015. Voltage stability and reactive power sharing in inverter-based microgrids with consensus-based distributed voltage control. *IEEE Transactions on Control Systems Technology*, 24(1), pp.96-109.

[3] Simpson-Porco, J.W., Dörfler, F. and Bullo, F., 2016. Voltage stabilization in microgrids via quadratic droop control. *IEEE Transactions on Automatic Control*, 62(3), pp.1239-1253.

[4] Wang, B., Sechilariu, M. and Locment, F., 2012. Intelligent DC microgrid with smart grid communications: Control strategy consideration and design. *IEEE transactions on smart grid*, 3(4), pp.2148-2156.

[5] Guerrero, J.M., Vasquez, J.C., Matas, J., De Vicuña, L.G. and Castilla, M., 2010. Hierarchical control of droop-controlled AC and DC microgrids—A general approach toward standardization. *IEEE Transactions on industrial electronics*, 58(1), pp.158-172.

[6] Lu, X., Guerrero, J.M., Sun, K. and Vasquez, J.C., 2013. An improved droop control method for dc microgrids based on low bandwidth communication with dc bus voltage restoration and enhanced current sharing accuracy. *IEEE Transactions on Power Electronics*, 29(4), pp.1800-1812.

[7] Molzahn, D.K., Dörfler, F., Sandberg, H., Low, S.H., Chakrabarti, S., Baldick, R. and Lavaei, J., 2017. A survey of distributed optimization and control algorithms for electric power systems. *IEEE Transactions on Smart Grid*, 8(6), pp.2941-2962.

[8] Rivero, S. and Ferrari-Trecate, G., 2012. Tube-based distributed control of linear constrained systems. *Automatica*, 48(11), pp.2860-2865.

[9] Farina, M. and Scattolini, R., 2012. Distributed predictive control: A non-cooperative algorithm with neighbor-to-neighbor communication for linear systems. *Automatica*, 48(6), pp.1088-1096.

[10] Ferreira, P.D., Carvalho, P.M., Ferreira, L.A. and Ilic, M.D., 2012. Distributed energy resources integration challenges in low-voltage networks: Voltage control limitations and risk of cascading. *IEEE Transactions on Sustainable Energy*, 4(1), pp.82-88.

[11] Zhang, F., Duan, X., Liao, M., Zou, J. and Liu, Z., 2019. Statistical analysis of switching overvoltages in UHV transmission lines with a controlled switching. *IET Generation, Transmission & Distribution*, 13(21), pp.4998-5004.

[12] Bottrell, N. and Green, T.C., 2013. Comparison of current-limiting strategies during fault ride-through of inverters to prevent latch-up and wind-up. *IEEE Transactions on Power Electronics*, 29(7), pp.3786-3797.

[13] Konstantopoulos, G.C. and Baldvieso-Monasterios, P.R., 2020. State-limiting PID controller for a class of nonlinear systems with constant uncertainties. *International Journal of Robust and Nonlinear Control*, 30(5), pp.1770-1787.

[14] Baldvieso-Monasterios, P.R. and Trodden, P.A., 2018. Model predictive control of linear systems with preview information: Feasibility, stability, and inherent robustness. *IEEE Transactions on Automatic Control*, 64(9), pp.3831-3838.

[15] Braitor, A.C., Konstantopoulos, G.C. and Kadiramanathan, V., 2020, September. Novel droop control design for overvoltage protection of DC microgrids with a constant power load. In 2020 28th Mediterranean Conference on Control and Automation (MED) (pp. 875-880). IEEE.

[16] Dörfler, F. and Bullo, F., 2012. Synchronization and transient stability in power networks and nonuniform Kuramoto oscillators. *SIAM Journal on Control and Optimization*, 50(3), pp.1616-1642.

[17] Vorobev, P., Huang, P.H., Al Hosani, M., Kirtley, J.L. and Turitsyn, K., 2017, December. A framework for development of universal rules for microgrids stability and control. In 2017 IEEE 56th Annual Conference on Decision and Control (CDC) (pp. 5125-5130). IEEE.

[18] Khalil, H.K. and Grizzle, J.W., 2002. *Nonlinear systems* (Vol. 3). Upper Saddle River, NJ: Prentice hall.

[19] Rawlings, J.B., Bonn e, D., Jorgensen, J.B., Venkat, A.N. and Jorgensen, S.B., 2008. Unreachable setpoints in model predictive control. *IEEE Transactions on Automatic Control*, 53(9), pp.2209-2215.

[20] Mayne, D.Q. and Michalska, H., 1988, December. Receding horizon control of nonlinear systems. In Proceedings of the 27th IEEE Conference on Decision and Control (pp. 464-465). IEEE.